Full mimicking of coronary hemodynamics for ex-vivo stimulation of human saphenous veins

Marco Piola[1,*,#], Matthijs Ruiter[2,#], Riccardo Vismara[1], Valeria Mastrullo[2], Marco Agrifoglio[3], Marco Zanobini[4], Maurizio Pesce[2] Monica Soncini[1] and Gianfranco Beniamino Fiore[1]

[1] Dipartimento di Elettronica, Informazione e Bioingegneria, Politecnico di Milano, , P.zza Leonardo da Vinci 32, 20133, Milan, Italy;

[2] Unità di Ingegneria Tissutale, Centro Cardiologico Monzino-IRCCS, Via Parea 4, 20138, Milan, Italy;

[3] Dipartimento di Scienze Cliniche e di Comunità, Università di Milano, Via Parea 4, 20138, Milan, Italy.

[4] Divisione Di Cardiochirurgia, Centro Cardiologico Monzino-IRCCS, Via Parea 4, 20138, Milan, Italy

# Both authors contributed equally to this work

Running title: *Ex vivo* pulsatile stimulation of human saphenous veins

*corresponding author:

Marco Piola, PhD. – Address: Dipartimento di Elettronica, Informazione e Bioingegneria, Politecnico di Milano, P.zza Leonardo da Vinci, 32, 20133 Milano, Italy, TEL: +39 02 2399 4144, FAX: +39 02 2399 3360, E-mail: marco.piola@polimi.it

This is the peer reviewed version of the following article Piola M., Ruiter M., Vismara R., Mastrullo V., Agrifoglio M., Zanobini M., Pesce M., Soncini M., Fiore G.B. Full Mimicking of Coronary Hemodynamics for Ex-Vivo Stimulation of Human Saphenous Veins. Annals of Biomedical Engineering. Volume 45, Issue 4, Pages: 884-897, April 2017, doi: 10.1007/s10439-016-1747-7, which has been published in final form at Springer Nature web site (https://link.springer.com/article/10.1007%2Fs10439-016-1747-7 - citeas). This article may be used for non-commercial purposes in accordance with Springer Nature Terms and Conditions for Self-Archiving (https://www.springer.com/gp/open-access/authors-rights/self-archiving-policy/2124).

Abstract

After coronary artery bypass grafting, structural modifications of the saphenous vein wall lead to lumen narrowing in response to the altered hemodynamic conditions. Here we present the design of a novel *ex vivo* culture system conceived for mimicking central coronary artery hemodynamics, and we report the results of biomechanical stimulation experiments using human saphenous vein samples. The novel pulsatile system used an aortic-like pressure for forcing a time-dependent coronary-like resistance to obtain the corresponding coronary-like flow rate. The obtained pulsatile pressures and flow rates (diastolic/systolic: 80/120mmHg and 200/100 ml/min, respectively) showed a reliable mimicking of the complex coronary hemodynamic environment. Saphenous vein segments from patients undergoing coronary artery bypass grafting (n=12) were subjected to stimulation in our bioreactor with coronary pulsatile pressure/flow patterns or with venous-like perfusion. After 7-day stimulation, SVs were fixed and stained for morphometric evaluation and immunofluorescence. Results were compared with untreated segments of the same veins. Morphometric and immunofluorescence analysis revealed that 7 days of pulsatile stimulation: *i*) did not affect integrity of the vessel wall and lumen perimeter; *ii*) significantly decreased both intima and media thickness, and *iii*) lead to partial endothelial denudation, and *iv*) induced apoptosis in the vessel wall. These data are consistent with the early vessel remodeling events involved in venous bypass adaptation to arterial flow/pressure patterns. The pulsatile system proved to be a suitable device to identify *ex vivo* mechanical cues leading to graft adaptation.

Keywords: *Coronary Flow Rate; Pulsatile Pressure; Saphenous Vein Graft Disease; Ex Vivo Platform; Wall Remodeling*

1. Introduction

The autologous saphenous vein (SV) is commonly used as a conduit to treat atherosclerotic lesions in coronary artery bypass graft surgery (CABG). However, according to follow-up studies, the average 10-year patency rate of human SV grafts is reduced to 50%-60%, due to an uncontrolled proliferation of smooth muscle cells (SMC) in the intima[1], a process called intima hyperplasia[2, 3]. This event dramatically reduces patient survival, especially when treated for multi-vessel coronary artery disease[4].

The late failure of SV grafts appears to be linked to early modifications in the vessel mechano-biological status[5]. After engraftment into the coronary circulation, the SV is exposed to elevated wall shear stress (WSS) and pressure-related wall strain with respect to its native physiological conditions. Briefly, in their natural bed SVs are subjected to a quasi-steady, low flow pattern, and to low WSS (0.1-0.6 Pa)[6] and transmural pressure loads (10-20 mmHg)[7-9]. By contrast, after CABG surgery SV segments are exposed to pulsatile flow (mean flow rate up to 250 ml/min), high WSS in the range of 0.75-2.25 Pa, and a systolic/diastolic pressure of approximately 120/80 mmHg[10]. These non-physiologic conditions lead to sudden modifications in the endothelial cell (EC) and SMC response, and to changes in the vessel wall structure, that ultimately result in progressive graft occlusion due to neo-intima formation. Pulsatile wall strain and WSS are considered the main biomechanical cues involved in SV remodeling. Elevated WSS, acting on the ECs, may lead to an increase in nitric oxide (NO) release due to a WSS-dependent elevation of endothelial NO synthase expression, and alteration of the intimal layer. As a consequence of the endothelial denudation and EC apoptosis, the basal lamina is exposed to the circulating blood, and this promotes the activation of the inflammatory cascade[5]. Pulsatile strain, acting on the SV wall, may play a pro-pathological effect, contributing to mechanical rupture of the intimal layer, and leading to an abnormal strain experienced by SMCs[7]. Indeed, SMC response to this stimulus is characterized by apoptosis as an early event, followed by SMC proliferation and migration from the media to the intima during the first weeks[11, 12].

Ex vivo vessel culture systems (EVCSs) offer the possibility to study the effects of pulsatile WSS and/or pressure, under well-controlled and strictly reproducible biomechanical conditions[10]. These systems may also offer the possibility to discriminate between the effects caused by WSS[13, 14] with respect to those generated by the pure pulsatile pressure[15, 16], representing a unique insight into vascular adaptation to a combination of stimuli. Few efforts have been spent up to now to exploit the potential of EVCSs towards a high-fidelity *ex vivo* replication of the hemodynamic factors affecting SV behavior in CABG.

In order to investigate the early events triggered by the modifications in hemodynamic load acting in the human SV after implantation into coronary position, we have developed an EVCS that enables stimulating human SV samples with a pressure/flow pattern mimicking that of the coronary circulation, *i.e.* a sphygmoid pulsatile pressure, oscillating between a diastolic minimum and a systolic maximum, in counter-phase with a pulsatile flow rate, oscillating between a systolic minimum and a diastolic maximum. Compared to our previously published studies[15, 16], this EVCS stimulated SV segments with a fully realistic coronary-like hemodynamics with the aim of dissecting the biomechanical cues involved in the human disease.

2. Materials and Methods

2.1 Design specifications of the system

The new EVCS consisted of a culture chamber hosting a human SV segment, coupled with an active hydraulic circuit (coronary pulse duplicator, CPD) for generating coronary-like pulsatile flow patterns in the cultured vessel.

The culture chamber was a modified version of our previous device[15, 16], the general design specifications, material choice and manufacturing methods of which were described elsewhere[15, 17, 18]. Briefly, a mounting chassis enables hosting a human SV segment onto a couple of hollow connectors, thus creating a water-tight connection of the vessel lumen to an external stimulating circuit. Culture medium is flowed one-directional from the inlet to the outlet connectors in this

design. The mounting chassis, together with the hosted sample, is then dipped into a falcon tube which acts as a reservoir for the medium; shielding against contamination is achieved thanks to a sealed press-fit securing of the chassis into the falcon tube.

The design specifications for the CPD circuit, in turn, were related to the replication of central left coronary hemodynamics (refer to *Supplementary Materials Online* - paragraph 1 for further details): *i*) the pressure exerted in SVs used as grafts in the left coronary circulation substantially coincides with the aortic pressure waveform, *ii*) the cyclic contraction of the cardiac muscle generates a time-dependent flow/pressure relation, *iii*) the left coronary blood flow has a mean value equal to 175 ml/min (70% of the overall coronary flow rate), and *iv*) the peak flow in diastole is 2-3-fold the peak flow in systole (Figure 1A). The CPD was designed to grant these hydrodynamic features, together with other, not less important requisites related to practical laboratory usage: compactness, priming volume limitation, easy set-up, automated running and limitation of efforts and costs.

2.2 Design of the CPD-equipped EVCS

A schematic representation of the CPD-equipped EVCS is shown in figure 1B. The CPD system comprised three main components: *i*) a peristaltic pump equipped with a low-pass hydraulic filter for dampening its cyclical peristaltic disturbance, *ii*) a service impedance, *iii*) a coronary-like time-dependent impedance. While the coronary-like impedance acted as an afterload, placed in line with the SV culture chamber, the service impedance was placed in parallel, dynamically acting to yield the desired pressure-flow behavior in the SV hydraulic line (refer to *Supplementary Materials Online - paragraph 2* for further details).

The modified EVCS culture chamber (Figure 1C) had increased inflow and outflow cannulas (3.8 mm inner diameter, and length equal to 50 mm) with respect to our previous design[15, 16], to enable left coronary-like flow levels through the hosted SV sample. With such dimensioning, the flow fully develops along the inflow cannula, as calculated with classical formulas for laminar

flow[19]. In such a way, the sample lumen is fed by flow in the most controllable and smooth condition. The pressure/flow behavior of the new culture chamber was characterized under steady state regimen using an axial flow pump (Figure 1D) with a working fluid (3.2±0.09 cP viscosity) consisting of 55% sucrose (w/v) dissolved in distilled water. During experiments, flow rates ranging 40 to 240 ml/min, step 20 ml/min, were imposed and the resulting pressure drop across the chamber was recorded (Figure 1D, E).

The CPD circuit was dimensioned taking into account the hydraulic characteristics of the new culture chamber. As a general strategy, computer-aided design of the hydrodynamic circuitry was performed by lumped parameter modeling[20], running simulations with Simnon 3.0 (SSPA Maritime Consulting AB, Sweden) in order to achieve satisfying hemodynamic conditions. Figure 1F shows the lumped parameter model of the CPD circuit: *i)* dampening of the peristaltic pump was obtained with an R-C low-pass hydraulic filter; *ii)* the service impedance was realized with a single hydraulic compliance element; *iii)* the time-dependent coronary impedance behavior was obtained switching between a systolic and a diastolic resistance components (refer to *Supplementary Materials Online* for further details). Specifically, the service impedance was modeled in order to generate a sphygmoid-like pressure waveform as an input signal to the line comprising the culture chamber and the time-dependent coronary resistance. Different combinations of R and/or C lumped parameters were taken into account; the use of a single compliance element as the service impedance represented the best trade-off among the possible configurations, in terms of ease of realization, compactness, and low-priming volume.

2.3 Manufacturing of the CPD circuit

The coronary resistances were realized with cell-culture compatible tubing. Briefly, the inner diameter and the length of the tubes were dimensioned in order to fit the following requirements (refer to *Supplementary Materials Online - paragraph 2.1* for further details): *i*) guaranteeing a laminar flow within the resistance elements; *ii*) minimizing minor head losses across the resistance

elements; *iii*) minimizing the inductive and capacitive contributions, and *iv*) taking into account the hydraulic resistance of the EVCS culture chamber. The resulting systolic resistance consisted of a 750 mm-length tube with an inner diameter of 2.4 mm, while the diastolic resistance was a 100 mm-length tube with an inner diameter of 3.2 mm. Screw clamps were added in the systolic and diastolic circuits to enable additional resistance adjustment. Switching between the systolic and diastolic resistance was achieved by means of a solenoid pinch-valve (S306-02, SIRAI® Elettromeccanica, Italy). The pinch valve is connected to a PC equipped with an I/O board (NIDAQCard-6036E, National Instruments Corp.) and custom-made LabView software (National Instruments Corp., TX, USA), imposing the simulated cardiac frequency and the systole/diastole time ratio.

Regarding the service compliance, numerical simulations suggested an optimal value equal to 0.01 ml/mmHg; this component was realized by using a properly dimensioned component based on compression and expansion of air within a chamber (air volume 13.5 ml) (refer to *Supplementary material online – paragraph 2.2* for further details).

Concerning the low-pass RC-hydraulic filter, simulations suggested a cutoff frequency equal to 0.05 Hz. The filter resistance was set higher than the systolic and diastolic ones, to ensure a good decoupling of the filtering stage from the remaining CPD circuit. Optimal results were obtained from simulations with a filter resistance equal to 120 mmHg s/ml. The requested filter compliance was thus equal to 0.025 ml/mmHg (Table S1). The filter resistance was realized with four parallel silicone tubes (inner diameter 0.6 mm, Platinum Cured Silicone, Cole Parmer, Vernon Hills, IL). Silicone tubes (inner diameter of 3.2 mm, wall thickness of 0.8 mm and length of 2500 mm, Platinum Cured Silicone, Cole Parmer, Vernon Hills, IL) were also used for the filter compliance (*Supplementary material online – paragraph 2.3*), thus obtaining the oxygenating elements for the culture medium as well[15, 21].

2.4 Functional assessment for testing the performance of the EVCS platform

Preliminary experiments were performed to verify the hemodynamics of the developed CPD-equipped EVCS under pulsatile flow, with a blood analog fluid and a silicone tube used as a SV substitute (Figure 1D). The coronary flow and pressure signals were acquired at the inlet of the culture chamber (P1); pressure was acquired along the SV substitute (P2) through purpose-developed pressure ports (Figure 1D). A transit-time ultrasound flow meter (HT110R, Transonic System Inc., Ithaca, NJ, USA) equipped with a ¼" probe was used for flow rate and two pressure transducers (Press-S-000, PendoTECH, NJ, USA) were used for pressure. Signals were acquired at 200 Hz via a PC equipped with an I/O board (NIDAQCard-6036E, National Instruments Corp.), with a LabView-based software (National Instruments Corp., TX, USA).

2.5 Human SVs preparation

The employment of human SV segments - discarded after the end of bypass surgery interventions, and accompanied by a written informed consent - was approved by the Ethical Committee of the Centro Cardiologico Monzino. The study conforms to the ethical standards laid down in the 1964 Declaration of Helsinki and its later amendments. Surplus segments of SV were obtained from 12 randomly selected patients undergoing CABG surgery (average age 69.8±14.5). SV samples were gently harvested to avoid vasospasm and dilatation, and preserve as much as possible endothelial, medial and adventitial integrity. Harvesting and manipulation procedures were the same for all the treated samples. The distal end of each SV segment was cannulated in the operating room, thus allowing the identification of the flow direction and side branches were ligated. The SV sample was immediately stored at 4°C in Dulbecco Modified Eagle's Medium (DMEM) supplemented with 10% Fetal Bovine Serum (FBS), 1% L-Glutamine, and 1% Penicillin/Streptomycin and divided in two fragments. A 5-cm-long segment was mounted in the EVCS and exposed to CABG-like or venous-like perfusion (VP) stimulation. The remaining fragment was fixed in 10% neutral buffered formalin overnight and used as control sample (Native groups: CABG-t0 and VP-t0). The SV segments were cultured for 7 days under CABG conditions

(CABG-t7, n=6, luminal pressure: 80 - 120 mmHg; pulse frequency: 1 Hz; mean flow rate: ~150-170 ml/min), or VP conditions (VP-t7, n=6, steady flow with luminal pressure: 5 mmHg; flow rate: 3 ml/min). In all experiments, the distal end of each sample was mounted onto the inlet connector of the culture chamber after gently removing the existing cannula. Then the proximal end was mounted onto the outlet connector, with an axial pre-tensioning of about 10%. Other details related to the SV mounting procedure are described in our previous papers[15-17].

2.6 Functional assessment for testing the performance of the EVCS platform using SV specimens

The CPD-equipped EVCS was filled with DMEM with 10% Fetal Bovine Serum (FBS), 1% L-Glutamine, 1% Penicillin/Streptomycin, and 3.5% of dextran (450000-650000 kDa, Sigma). The addition of dextran led to a medium viscosity of 3.07±0.07 cP. In the VP group, DMEM with 10% Fetal Bovine Serum (FBS), 1% L-Glutamine, 1% Penicillin/Streptomycin was used.

In the CABG group, the CPD pulse was enabled, then flow rate was gently increased until a sphygmoid-like pressure wave was reached and the resulting flow/pressure curves were recorded. The resulting values for WSS were 2.6 Pa and 1.3 Pa during the diastole and systole, respectively, as estimated using the Haagen-Poiseuille equation ($WSS = {}^{4\mu Q}/_{\pi r^3}$). Indeed, assuming a typical SV radius of 1.7 mm, 200/100 ml/min diastolic/systolic peak flow rates, and 1 Hz pulse frequency, the Womersley number equals 2.4, a value which indicates viscous effects are dominant, hence WSS can be calculated with a quasi-steady approach[22-24]. The system was kept in the incubator at 37°C and 5% CO_2 for a culture period of 7 days, the culture medium was partially changed at day 3. During the 7-day of CABG experiment, pressure and flow rate were monitored daily and recorded every 3 days. At the end of the stimulation period, SV samples (of both group) were extracted and the central portion of each sample was immediately fixed in 10% neutral buffered formalin overnight for the following analyses.

2.7 SV morphology and morphometry

Fixed tissue rings before and after stimulation (VP-t0: n=6; VP-t7: n=6; CABG-t0: n=6; CABG-t7: n = 6) (VP: n=6; and CABG: n=6) were embedded in paraffin and cut (5 μm) using a rotary microtome. Sections were stained with hematoxylin and eosin (H&E) for general histology, with Masson's trichrome (MT) staining for evaluation of the lumen and media and with Weigert van Gieson (WvG) for delineation of the intima (all from Bio-Optica Milano SpA, Italy). Digital images were acquired using a light microscope (AxioVision Bio Software, Carl Zeiss, Germany) at a magnification of 10x. Lumen and media perimeters were assessed using ImageJ (version 1.46r, National Institutes of Health, USA). Wall thickness was determined as the mean distance of 24 measurements per section from the outer limit of the lumen to the outer limit of the media (AxioVision Bio Software), identified by MT. Intima thickness was defined as the mean distance of 24 measurements per section from the outer limit of the lumen to the internal elastic lamina, identified by WvG. Media thickness was defined as the difference between wall thickness and intima thickness.

2.8 Immunofluorescence staining

Immunofluorescence (IF) staining for SMCs and ECs were performed on sections before and after stimulation (VP at t0 and t7: n=3; and CABG at t0 and t7: n=6). After blocking, with 3% bovine serum albumin (BSA, Sigma Aldrich), sections were incubated (4˚C, overnight) with mouse anti-human αSMA (1:500, Dako) for labeling SMCs and with goat anti-human CD31 (1:200, Santa Cruz) and rabbit anti-human vWF (1:500, Dako) for labeling ECs. Sections were subsequently incubated with Alexa Fluor 488 anti-mouse, Alexa Fluor 546 anti-goat, and Alexa Fluor 633 anti-rabbit (1:500, Invitrogen) secondary antibodies for 1 h at room temperature. Nuclei were counterstained with DAPI (Vector Laboratories, CA, USA). Digital images were obtained using a multicolor detection protocol in a LSM-710 confocal scanning microscope (Carl Zeiss, Germany). In order to evaluate the linear density of ECs lining the vessel wall on the luminal side,$CD31^+$ cells

nuclei were counted with ImageJ in 2 different fields of each section (VP: n=3 and CABG: n=4) and expressed as number of $CD31^+$ nuclei per unit lumen circumferential length [CD31+ cells /μm].

2.9 Assessment of proliferation and apoptosis

In order to quantify proliferation of cells throughout the vessel wall, immunohistochemical staining of Ki67 was performed in 4 sections of each condition (VP: n=4 and CABG: n=4). After heat-induced epitope retrieval (citrate buffer, 98°C, 10 minutes) and quenching (hydrogen peroxide 0.6%, 15 minutes), aspecific binding was blocked with 3% BSA and sections were incubated overnight at 4˚C with an antibody against Ki67 (1:100, rabbit polyclonal, Invitrogen). Subsequently, sections were incubated with a secondary antibody for 1 hour (goat anti-rabbit HRP, Invitrogen, 1:100), after which staining was developed using the ImmPACT DAB Peroxidase Substrate kit (Vector Laboratories). Sections were counterstained with hematoxylin.

Determination of apoptosis was obtained by performing a TUNEL staining (DeadEnd Colorimetric TUNEL assay, Promega Italy). From each experimental condition 3 sections (VP: n=3 and CABG: n=3) were stained according to the manufacturer's protocol, followed by a hematoxylin counterstain. Ki67/ TUNEL-positive and total cells were counted manually using Image-J software (Version 1.47f-sofware for Java, National Institutes of Health, USA) in 4 randomly selected microscopic fields (20x).

3.0 Statistical analysis

Data are presented as mean±standard error. Morphometric measurements, proliferation and apoptosis and IF endothelial lining, before (t0) *vs*. after stimulation (t7) were analyzed by paired *t* test, while unpaired *t* test was used in VP *vs* CABG and in the t0 *vs* t0 analysis. A p value <0.05 was considered statistically significant in both tests. Statistical analysis was performed using GraphPad Prism 5.

3. Results

3.1 Assembly of the EVCS platform

In figure 2 the prototype of CPD-equipped EVCS is shown. The assembled culture chamber (Figure 2A) was connected to the CPD circuit, and to an additional falcon tube, acting as additional reservoir for culture medium (Figure 2B). The culture chamber containing the SV sample was immediately filled with culture medium in order to maintain the SV tissue wet and hydrated (Figure 2C); then the systolic and diastolic resistances were filled (Figure 2D). For filling the entire CPD-equipped-EVCS circuit 130 ml of culture medium was used. The coronary resistances were finally connected to the pinch valve, switching between systolic and diastolic resistance, (Figure 2E), the system was placed in the incubator (Figure 2F) and connected to the peristatic pump and to the flow meter. Pressure and flow rate signals were acquired close to the inflow port (P1) of the culture chamber. A video (Video S1) of the CPD-equipped EVCS during stimulation of human SV in the incubator is reported in the *Supplementary material online* section.

3.2 Functional assessment of the CPD-equipped EVCS

The measured flow rate and pressure (Figure 3A thick line) were compared to those reported in literature (Figure 3A, thin line)[25, 26], demonstrating a good correspondence with the physiological curves (i.e., the peak flow rate during diastole being approximately 2.5-fold the flow during systole, and coronary pressure and flow rate waveforms in counter-phase) as confirmed by the RMSE analysis (Figure 3A).

Figure 3B summarizes the results of the functional experiments performed using the silicone vessel substitute (Figure 1D) under pulsatile flow regimen. The traces in figure 3B show almost overlapping values of P1 (red) and P2 (blue), thus indicating P1 as good candidate to estimate the luminal pressure.

Figure 3C depicts the flow and pressure (in P1) stimulation patterns applied to the human SV during the 7-days experiments. A good reproducibility was observed among six experimental runs,

with a mean coronary flow rate of 156.4±6.9 ml/min and a mean pressure value equal to 95±6.2 mmHg (values obtained on day 0 of each run, with a frequency of 1 Hz and a systolic time equal to 0.35 s). In addition, pressure and flow rate remained quite stable during the entire stimulation period with an acceptable decrease of the mean pressure (with respect to day 0) of 1.2% and 3.4% at day 3 and day 7, respectively; consistently, the mean flow rate decreased 0.4% and 3.3% at day 3 and day 7, respectively.

3.3 SV remodeling after 7 days of pulsatile stimulation in the CPD-equipped EVCS

Figure 4 offers a qualitative representation of the morphologic changes occurring due to the application of a full CABG-like hemodynamic pattern or low flow/pressure perfusion (VP), evaluated with histological images before and after treatment in the bioreactor. H&E (Figure 4A, B and C), MT (Figure 4D, E and F) and WvG (Figure 4G, H and I) staining enable assessing the morphometric features, the cellular organization of the media and the intima thickness, respectively. In line with our previous reports[15-17], the stimulated human SV segments did not display any signs of tissue degeneration nor swelling. As shown by the different staining procedures, CABG-like stimulation and VP perfusion neither affected the integrity of the vessel wall and lumen perimeter, nor altered collagen content. The organization of the internal elastic lamina (Figure 4G, H and I, white arrows) was visible in all sections, not as a continuous layer but identifiable in the majority of the transversal sections perimeter. Integrity of the lamina was similar in native, CABG and VP groups. Morphometric analysis on MT and WvG stained sections (Figure 4J) revealed that both intima thickness (CABG - t7: 33.5±4.2; t0 : 39.2±5.1 μm; p=0.03) and media thickness (CABG – t7: 226±16; t0: 339±34 μm; p=0.01) decreased significantly after stimulation, resulting in significantly reduced wall thickness (CABG - t7: 260±19; t0: 378±36 μm; p=0.01) at day 7. These structural changes were not detected in the VP group (Figure 4J), confirming that the application of CABG stimulation for 7 days was sufficient to induce geometric modifications in the SV.

Cells proliferation and apoptosis were investigated by Ki67 and TUNEL assays (Figure 5), respectively.. Figures 5 A, B and C show representative $Ki67^{+}$/hematoxylin stained sections of Native, VP and CABG samples. Similarly, representative TUNEL/hematoxylin stained sections of Native, VP and CABG samples are shown in Figure 5 D, E and F. Quantification of cell proliferation (Figure 5G) and apoptosis (Figure 5F) indicate that, while apoptosis was significantly increased by stimulation, both in the CABG and VP group, a trend towards increased cell proliferation was observed in CABG group.

Vessel wall cellular composition was investigated by IF (Figure 6), using antibodies recognizing SMC marker αSMA and EC markers vWF and CD31. The distribution of αSMA showed a similar arrangement of the cells between Native and stimulated (CABG, and VP) samples, with SMCs mostly aligned in several layers in a circumferential direction in the media and longitudinally in the intima (Figure 6 A, B and C, low magnification). The intima was composed mainly of SMCs, with a lining of ECs on the luminal side. The presence of EC markers CD31 and vWF on the luminal side of the vessel wall after stimulation indicated the presence of ECs in CABG and VP segments. Instead, pulsatile stimulation resulted in a trend towards a reduction of the endothelial lining in the CABG group (CABG – t7: 0.007±0.001 CD31+ cells /μm; t0: 0.024±0.007 CD31+ cells /μm; p=0.07, Figure 6G, left panel). No significant differences are reported for VP *vs.* untreated samples (VP – t7: 0.004±0.001 CD31+ cells /μm; t0 :0.008±0.003 CD31+ cells/μm; p=0.2, Figure 6G, right panel). This suggests that the endothelial layer was maintained, at least in part, despite the high mechanical load in terms of WSS and circumferential strain applied in CABG stimulation.

4. Discussion and conclusion

CABG is carried out worldwide as a standard therapy to re-vascularize the ischemic myocardium, although a large number of patients yearly require re-hospitalization because of the loss of patency of autologous SV grafts[27, 28]. Apparently, there is a strong need for experimental

tools and procedures to unravel the biological causes of this unresolved issue. Experimental studies on vein graft disease (VGD) may benefit from the fact that CABG surgery most often involves the discarding of surplus SV segments, which may be made available to the biological laboratory. The use of such invaluable human samples for *ex-vivo* organ culture experiments requires common efforts of surgeons, vascular biologists and bioengineers.

In the present study, the use of bioengineering tools and vascular biology expertise provided a valuable strategy for studying the early remodeling events activated by exposure of the human SV to highly biomimetic arterial-like conditions. The adopted approach enabled us to investigate *ex vivo* the effects of the altered flow and pressure conditions experienced by the human SV after CABG using a novel pulsatile EVCS, specifically conceived for *ex vivo* culture experiments.

The *ex vivo* culture system was conceived to be a user-friendly and cost-effective device with respect to most of the state-of-the-art solutions, which are often based on the adaptation of cumbersome mechanical work-bench simulators[29, 30]. We tried to overcome some of the limitations of most previous hemodynamic-based bioreactors implementing a number of architectural and technical solutions to simplify the fluidic layout, the control system and the related equipment. In addition, compactness was considered a primary requisite, which yielded to an overall priming volume to 130 ml, substantially lower than the 5000 ml and 500 ml reported by Voisard and colleagues and Longchamp and colleagues, respectively[31, 32] . This aspect is particularly important for systems aimed at hosting *ex vivo* organ cultures, considering the need to limit the cost of reagents or drugs used for culturing the samples. Together with limited encumbrances and volumes, still a high-level performance was obtained in terms of replication of coronary hemodynamics. Indeed our functional tests revealed the EVCS was capable of replicating the so-called 'paradox' behavior of central left coronary circulation hemodynamics, consisting in pressure and flow peaks occurring in counter-phase, with a maximum flow rate occurring during the diastole. To our knowledge, none of the state-of-the-art pulsed-flow duplicators[29, 30, 33] are able to mimic with good fidelity the complexity of the coronary hemodynamic environment.

Full CABG-like stimulation of human SVs in this novel pulsatile platform resulted in geometric remodeling of the vessel wall. Our data (CABG-t7 group vs. t0) indicated a constant value of the luminal perimeter and a clear thinning of the SV wall. These data are compliant with those reported in several recent articles processing human SVs *in vitro*. In particular, the observed medial thinning is in accordance with findings by Longchamp and colleagues[32] and with our previous work, in which SVs were exposed to CABG-like pressure loads *ex vivo*[15, 16]. By contrast, no increase in lumen perimeter was evidenced after 7 days of stimulation, whereas a relevant increase in perimeter was reported in our previous work with pressure-only stimulation[15, 16]. A possible explanation of this finding is that addition of an arterial flow with a blood-like viscosity may have a balancing role to the effect induced by pressure-only stimulation due to a WSS effect preventing the outward remodeling. In this regard it has to be noted that unraveling the mechanism of remodeling is not a simple task, since many opposing and interacting factors are involved, as reviewed before[34]. It is well known that WSS induces the release of nitric oxide, a potent vasodilator which is also involved in vascular remodeling[35, 36]. On the other hand, stretch upregulates expression of endothelin-1, which is predominantly a vasoconstrictor agent, implicated in the development of hypertension[37]. In addition, reactive oxygen species are released and matrix metalloproteinases are upregulated in response to flow, oxidative stress and mechanical injury [16, 38, 39]. Finally, *in vivo* these cues are supported by inflammatory mediators, and homing of circulatory monocyte-derived cells, which are mechanisms strongly coupled to the mechanical induced adaptation/remodeling.

During CABG operations, certain damage to vein grafts is unavoidable. Vasa vasorum and nerves are cut, both during harvest and grafting, and endothelium and adventitia inadvertently become damaged[40, 41]. In the new environment, the high flow and pressure may pose further damage on the individual cells and the structural integrity of the vessel. In this respect, the EVCS platform that was employed in the present report appears to be a good representation of the flow/pressure patterns typical of the coronary hemodynamics. Typically, vein arterialization is characterized by apoptosis in the first few days followed by an increase in proliferation, predominantly of SMCs[42, 43].

The exact time course differs among the different animal models used. In the present work, CABG-like stimulation of human samples resulted in an increase in apoptosis after 7 days, in accordance with previous reports. Proliferation however, showed only a trend towards an increase after 7 days of stimulation, and was not significantly different. Probably, 7 days was not the optimal time point for determining proliferation. Inclusion of more time points would be interesting to explore the proliferation and apoptosis patterns in human SV remodeling; however, this clearly falls beyond the scope of the present study. The endothelial monolayer was relatively preserved, and the orientation of the SMCs was mostly circumferential in the media, and longitudinal in the intima. Intimal hyperplasia is well described in clinical and preclinical studies in the context of vein graft disease, although the underlying mechanisms are yet to be unveiled[44, 45]. However, in *ex vivo* studies intimal hyperplasia is not always apparent, depending on the nature and duration of the stimulation[31, 32]. Furthermore, in studies using patient material, patient age, primary disease and co-morbidities affect the initial intima condition. In this respect, it has to be noted that the vein segments used in the present study were obtained from aged patients undergoing a CABG operation. It is then possible that considerable modifications of the vessel structure might have been already present due to aging and risk conditions, and that this was balanced in the EVCS by the applied WSS, which is known to have an atheroprotective effect.

In summary, the data presented here support the proof of concept for a novel CPD-equipped EVCS tailored to provide valuable insights in the process and time course of vein graft remodeling and disease. In perspective, this device will enable us to perform more observational and mechanistic studies (long term experiments are currently ongoing) to shed light onto the molecular and cellular events involved in the SV pathological remodeling in a realistic and strictly controlled biomechanical environment.

Acknowledgments

This work was supported by the Italian Ministry of Health research Project RF-2011-02346867. The authors would like to thank Dr. Emilio Savoldelli for his support during the preliminary design of the CPD circuit and Dr. Francesco Sturla for his support with MATLAB.

Disclosure Statement

The authors declare no conflict of interest to disclose.

References

1. Owens, C. D., Adaptive changes in autogenous vein grafts for arterial reconstruction: clinical implications. *J Vasc Surg.* 51:736-46, 2010.
2. Parang, P.,R. Arora, Coronary vein graft disease: pathogenesis and prevention. *Can J Cardiol.* 25:57-62, 2009.
3. Kim, F. Y., G. Marhefka, N. J. Ruggiero, S. Adams,D. J. Whellan, Saphenous vein graft disease: review of pathophysiology, prevention, and treatment. *Cardiol Rev.* 21:101-9, 2013.
4. Zacharias, A., T. A. Schwann, C. J. Riordan, S. J. Durham, A. S. Shah,R. H. Habib, Late results of conventional versus all-arterial revascularization based on internal thoracic and radial artery grafting. *Ann Thorac Surg.* 87:19-26 e2, 2009.
5. Muto, A., L. Model, K. Ziegler, S. D. D. Eghbalieh,A. Dardik, Mechanisms of Vein Graft Adaptation to the Arterial Circulation. *Circulation Journal.* 74:1501-1512, 2010.
6. Malek, A. M., S. L. Alper,S. Izumo, Hemodynamic shear stress and its role in atherosclerosis. *JAMA.* 282:2035-42, 1999.
7. Ochsner, A., Jr., R. Colp, Jr.,G. E. Burch, Normal blood pressure in the superficial venous system of man at rest in the supine position. *Circulation.* 3:674-80, 1951.
8. Stick, C., U. Hiedl,E. Witzleb, Venous pressure in the saphenous vein near the ankle during changes in posture and exercise at different ambient temperatures. *Eur J Appl Physiol Occup Physiol.* 66:434-8, 1993.
9. Meissner, M. H., G. Moneta, K. Burnand, P. Gloviczki, J. M. Lohr, F. Lurie, M. A. Mattos, R. B. McLafferty, G. Mozes, R. B. Rutherford, F. Padberg,D. S. Sumner, The hemodynamics and diagnosis of venous disease. *J Vasc Surg.* 46 Suppl S:4S-24S, 2007.
10. Piola, M., M. Soncini, F. Prandi, G. Polvani, G. Beniamino Fiore,M. Pesce, Tools and procedures for ex vivo vein arterialization, preconditioning and tissue engineering: a step forward to translation to combat the consequences of vascular graft remodeling. *Recent Pat Cardiovasc Drug Discov.* 7:186-95, 2012.
11. de Vries, M. R., K. H. Simons, J. W. Jukema, J. Braun,P. H. Quax, Vein graft failure: from pathophysiology to clinical outcomes. *Nat Rev Cardiol.* 13:451-70, 2016.
12. Liu, S. Q., Y. Y. Ruan, D. Tang, Y. C. Li, J. Goldman,L. Zhong, A possible role of initial cell death due to mechanical stretch in the regulation of subsequent cell proliferation in experimental vein grafts. *Biomech Model Mechanobiol.* 1:17-27, 2002.
13. Gusic, R. J., R. Myung, M. Petko, J. W. Gaynor,K. J. Gooch, Shear stress and pressure modulate saphenous vein remodeling ex vivo. *Journal of Biomechanics.* 38:1760-1769, 2005.
14. Miyakawa, A. A., L. A. O. Dallan, S. Lacchini, T. F. Borin,J. E. Krieger, Human Saphenous Vein Organ Culture under Controlled Hemodynamic Conditions. *Clinics.* 63:683-688, 2008.

15. Piola, M., F. Prandi, N. Bono, M. Soncini, E. Penza, M. Agrifoglio, G. Polvani, M. Pesce,G. B. Fiore, A compact and automated ex vivo vessel culture system for the pulsatile pressure conditioning of human saphenous veins. *J Tissue Eng Regen Med.* 10:E204-15, 2016.
16. Prandi, F., M. Piola, M. Soncini, C. Colussi, Y. D'Alessandra, E. Penza, M. Agrifoglio, M. C. Vinci, G. Polvani, C. Gaetano, G. B. Fiore,M. Pesce, Adventitial vessel growth and progenitor cells activation in an ex vivo culture system mimicking human saphenous vein wall strain after coronary artery bypass grafting. *PLoS One.* 10:e0117409, 2015.
17. Piola, M., F. Prandi, G. B. Fiore, M. Agrifoglio, G. Polvani, M. Pesce,M. Soncini, Human Saphenous Vein Response to Trans-wall Oxygen Gradients in a Novel Ex Vivo Conditioning Platform. *Ann Biomed Eng.* 44:1449-61, 2016.
18. Vismara, R., M. Soncini, G. Talò, L. Dainese, A. Guarino, A. Redaelli,G. B. Fiore, A Bioreactor with Compliance Monitoring for Heart Valve Grafts. *Annals of Biomedical Engineering.* 38:100-108, 2009.
19. Çengel, Y. A.,J. M. Cimbala, Fluid mechanics : fundamentals and applications. In *McGraw-Hill series in mechanical engineering*, McGraw-HillHigher Education,: Boston, 2006.
20. Milnor, W. R., *Hemodynamics*. Williams & Wilkins: Baltimore, 1982; p xiii, 390 p.
21. Piola, M., M. Soncini, M. Cantini, N. Sadr, G. Ferrario,G. B. Fiore, Design and functional testing of a multichamber perfusion platform for three-dimensional scaffolds. *ScientificWorldJournal.* 2013:123974, 2013.
22. Garcia, D., P. G. Camici, L. G. Durand, K. Rajappan, E. Gaillard, O. E. Rimoldi,P. Pibarot, Impairment of coronary flow reserve in aortic stenosis. *J Appl Physiol (1985).* 106:113-21, 2009.
23. Kajiya, F., S. Matsuoka, Y. Ogasawara, O. Hiramatsu, S. Kanazawa, Y. Wada, S. Tadaoka, K. Tsujioka, T. Fujiwara,M. Zamir, Velocity profiles and phasic flow patterns in the non-stenotic human left anterior descending coronary artery during cardiac surgery. *Cardiovasc Res.* 27:845-50, 1993.
24. Loudon, C.,A. Tordesillas, The use of the dimensionless Womersley number to characterize the unsteady nature of internal flow. *Journal of Theoretical Biology.* 191:63-78, 1998.
25. Guyton, A. C., *Textbook of medical physiology*. 2d ed.; W. B. Saunders Co.: Philadelphia, 1961; p 1181.
26. Berne, R. M., B. M. Koeppen,B. A. Stanton, *Berne & Levy physiology*. 6th ed.; Mosby/Elsevier: Philadelphia, PA, 2010; p xii, 836 p.
27. Harskamp, R. E., J. B. Williams, R. C. Hill, R. J. de Winter, J. H. Alexander,R. D. Lopes, Saphenous vein graft failure and clinical outcomes: toward a surrogate end point in patients following coronary artery bypass surgery? *Am Heart J.* 165:639-43, 2013.
28. Harskamp, R. E., M. A. Beijk, P. Damman, J. G. Tijssen, R. D. Lopes,R. J. de Winter, Prehospitalization antiplatelet therapy and outcomes after saphenous vein graft intervention. *Am J Cardiol.* 111:153-8, 2013.
29. Iwasaki, K., K. Kojima, S. Kodama, A. C. Paz, M. Chambers, M. Umezu,C. A. Vacanti, Bioengineered three-layered robust and elastic artery using hemodynamically-equivalent pulsatile bioreactor. *Circulation.* 118:S52-S57, 2008.
30. Narita, Y., K. Hata, H. Kagami, A. Usui, M. Ueda,Y. Ueda, Novel pulse duplicating bioreactor system for tissue-engineered vascular construct. *Tissue Eng.* 10:1224-33, 2004.
31. Voisard, R., E. Ramiz, R. Baur, I. Gastrock-Balitsch, H. Siebeneich, O. Frank, V. Hombach, A. Hannekum,B. Schumacher, Pulsed perfusion in a venous human organ culture model with a Windkessel function (pulsed perfusion venous HOC-model). *Med Sci Monit.* 16:523-9, 2010.
32. Longchamp, A., F. Alonso, C. Dubuis, F. Allagnat, X. Berard, P. Meda, F. Saucy, J. M. Corpataux, D. Sebastien,J. A. Haefliger, The use of external mesh reinforcement to reduce intimal hyperplasia and preserve the structure of human saphenous veins. *Biomaterials.* 35:2588-2599, 2014.

33. Punchard, M. A., C. Stenson-Cox, E. D. O'Cearbhaill, E. Lyons, S. Gundy, L. Murphy, A. Pandit, P. E. McHugh,V. Barron, Endothelial cell response to biomechanical forces under simulated vascular loading conditions. *Journal of Biomechanics.* 40:3146-3154, 2007.
34. Anwar, M. A., J. Shalhoub, C. S. Lim, M. S. Gohel,A. H. Davies, The effect of pressure-induced mechanical stretch on vascular wall differential gene expression. *J Vasc Res.* 49:463-78, 2012.
35. Vanhoutte, P. M., Y. Zhao, A. Xu,S. W. Leung, Thirty Years of Saying NO: Sources, Fate, Actions, and Misfortunes of the Endothelium-Derived Vasodilator Mediator. *Circ Res.* 119:375-96, 2016.
36. Ruiter, M. S., J. M. van Golde, N. C. Schaper, C. D. Stehouwer,M. S. Huijberts, Diabetes impairs arteriogenesis in the peripheral circulation: review of molecular mechanisms. *Clin Sci (Lond).* 119:225-38, 2010.
37. Cattaruzza, M., C. Dimigen, H. Ehrenreich,M. Hecker, Stretch-induced endothelin B receptor-mediated apoptosis in vascular smooth muscle cells. *FASEB J.* 14:991-8, 2000.
38. Mandel, E. R., C. Uchida, E. Nwadozi, A. Makki,T. L. Haas, Tissue Inhibitor of Metalloproteinase 1 Influences Vascular Adaptations to Chronic Alterations in Blood Flow. *J Cell Physiol.* 2016.
39. Gray, S. P., E. Di Marco, K. Kennedy, P. Chew, J. Okabe, A. El-Osta, A. C. Calkin, E. A. Biessen, R. M. Touyz, M. E. Cooper, H. H. Schmidt,K. A. Jandeleit-Dahm, Reactive Oxygen Species Can Provide Atheroprotection via NOX4-Dependent Inhibition of Inflammation and Vascular Remodeling. *Arterioscler Thromb Vasc Biol.* 36:295-307, 2016.
40. Tsui, J. C.,M. R. Dashwood, Recent strategies to reduce vein graft occlusion: a need to limit the effect of vascular damage. *Eur J Vasc Endovasc Surg.* 23:202-8, 2002.
41. Hashmi, S. F., B. Krishnamoorthy, W. R. Critchley, P. Walker, P. W. Bishop, R. V. Venkateswaran, J. E. Fildes,N. Yonan, Histological and immunohistochemical evaluation of human saphenous vein harvested by endoscopic and open conventional methods. *Interact Cardiovasc Thorac Surg.* 20:178-85, 2015.
42. Borin, T. F., A. A. Miyakawa, L. Cardoso, L. de Figueiredo Borges, G. A. Goncalves,J. E. Krieger, Apoptosis, cell proliferation and modulation of cyclin-dependent kinase inhibitor p21(cip1) in vascular remodelling during vein arterialization in the rat. *Int J Exp Pathol.* 90:328-37, 2009.
43. Westerband, A., D. Crouse, L. C. Richter, M. L. Aguirre, C. C. Wixon, D. C. James, J. L. Mills, G. C. Hunter,R. L. Heimark, Vein adaptation to arterialization in an experimental model. *J Vasc Surg.* 33:561-9, 2001.
44. Newby, A. C.,A. B. Zaltsman, Molecular mechanisms in intimal hyperplasia. *J Pathol.* 190:300-9, 2000.
45. Mitra, A. K., D. M. Gangahar,D. K. Agrawal, Cellular, molecular and immunological mechanisms in the pathophysiology of vein graft intimal hyperplasia. *Immunology and Cell Biology.* 84:115-24, 2006.

LEGEND OF THE FIGURES

Figure 1. A) Physiological aortic pressure (*upper panel*) and left coronary flow rate (*bottom panel*) curves re-drawn from Guyton & Hall (*Textbook of medical physiology*, 1961), and Berne & Levy *(Berne & Levy physiology*. 2010). Coronary blood flow is in counter-phase with respect to aortic pressure, meaning that it has a peak value during the diastolic phase. B) Schematic representation of the so-called coronary pulse duplicator (CPD) circuit, which constitutes the core hydrodynamic device of the novel *ex-vivo* vessel culture system (EVCS). The CPD consists of a pumping system with downstream filter impedance (*red*), the culture chamber (*black*) with the time-dependent coronary-like impedance downstream (*blue*) and a service impedance placed in a parallel line (*green*). C) Scheme of the modified culture chamber. A cannula with inner diameter of 1.6-mm was used for port *a*, while 3.8 mm inner diameter cannulas were used for ports *b*, *c*, *d* and *e*. Port *a* ensures atmospheric pressure within the chamber through a sterile HEPA filter, ports *b* (inflow) and *c* (outflow) are connected to the SV sample, ports *d* and *e* are connected to the outflow of the coronary impedance, and to aspiration line of the pump, respectively. D) Set-up adopted for the hydraulic characterization of the new culture chamber. A custom-made silicone tubular structure (*left panel*), equipped with two ports (P1 and P2) for pressure measurements, was used as SV substitute. E) Pressure drop *vs.* flow rate curve obtained for the culture chamber hydraulic characterization (linear fitting is adopted). F) Lumped parameter model of the CPD circuit (colors coherent with panel B): the hydraulic filter was implemented with an RC-low pass filter (*red*), the service impedance as a compliance element (*green)*, and the coronary impedance as a time-switched parallel of two resistances (*blue*).

Figure 2. CPD-equipped EVCS prototype during the assembling phase. A) The vessel housing chassis is inserted in the falcon reservoir and secured through a silicone O-ring gasket, resulting in a compact and isolated culture chamber. B) The culture chamber is then inserted in the CPD circuit, and connected to the pressure transducer and to a second falcon reservoir. C) The system is filled

with dextran-supplemented culture medium (3.07 cP viscosity) starting from the culture chamber. Then, the coronary resistance module is filled with medium (D) and tubes are hosted in the pinch valve (E-inset). F) Finally, the CPD-equipped EVCS is located in the incubator and connected to the peristaltic pump and the flow meter probe.

Figure 3. A) Comparison between measured data (thick line), and physiological (thin line) curves. RMSE analysis revealed a good correspondence between experimental measurements and physiological reference curves. B) Synchronous pressure and flow rate tracings acquired during the functional assessment campaign using a silicone vessel substitute. In the pressure graph, P1 is in blue while P2 is in red. C) Pressure (in P1) and flow rate data acquired during experiments in pulsatile conditions with human SV segments at 0, 3 and 7 days.

Figure 4. Representative SV tissue sections (10x) stained with H&E, Masson's trichrome and Weigert van Gieson staining of Native, VP and CABG samples. In all sections, *L* indicates the lumen of the samples. H&E staining shows general organization of the vein, which is similar in Native (A), VP (B) and CABG group (C). MT staining, indicating SMCs (cytoplasm) in red, collagen in blue, and nuclei in black, revealed no differences in structure, orientation and collagen content after stimulation in Native (D), VP (E) and CABG (F) group. Weigert van Gieson staining was used to identify the internal elastic lamina (indicated by white arrows), enabling intima thickness quantification in Native (G), VP (H) and CABG (I) samples. Quantification of the geometrical remodeling in CABG (t0 *vs* t7) and VP (t0 *vs* t7)samples (J). Wall thickness was significantly decreased after CABG stimulation (n=6), with no difference in lumen perimeter. In the vessel wall of CABG-treated samples, both intima and media thickness were significantly decreased by the stimulation. * indicates $p < 0.05$. No significant differences are detected in VP (n=6, t0 *vs* t7) samples. The direct comparison between CABG *vs* VP samples revealed a significant difference only in the lumen perimenter (unpaired *t*-test, $p = 0.0032$). A nonsignificant difference between t0 groups was also observed.

Figure 5. Representative SV tissue sections (10x) stained with Ki67/hematoxylin (A, B and C) and TUNEL/hematoxylin (D, E and F) of Native, VP and CABG samples. Note more abundant Ki-67^+ cells (red arrows) in CABG *vs.* Native and VP veins. Equally, note more abundant $TUNEL^+$ cells (black arrows) in CABG and VP *vs.* Native veins. Quantification of $Ki67^+$ and TUNEL positive cells is reported in G and H, respectively. The number of $TUNEL^+$ cells was significantly increased in CABG and VP samples. * indicates $p < 0.05$ by paired t-test (n=3 CABG samples; n=3 VP samples). Nonsignificant differences between CABG and VP, and between the two t0 groups were found for Ki67 and TUNEL markers.

Figure 6. Low magnification immunofluorescence (IF) of Native (A), VP (B) and CABG (C) samples. IF staining in CABG samples shows a predominantly circumferential alignment of SMCs (αSMA, in green) in the media, whereas intimal SMCs are mostly longitudinally oriented, both before and after conditioning. High magnification IF images show the presence of endothelial markers vWF (in white) and CD31 (in red) in Native (D), VP (E) and CABG (F) conditions. Interestingly, the number of $CD31^+$ nuclei seems to be decreased after CABG conditioning. *L* indicates lumen in all pictures. G) Linear density of $CD31^+$ cells lining the lumen showed a trend towards decrease after CABG stimulation (n = 4). However, the difference was not significant. No significant differences are reported for VP (t0 *vs.* t7*)* group. Also, nonsignificant differences between CABG and VP, and between the two t0 groups were found.

SUPPLEMENTARY FIGURE

Figure S1. A) Schematic of the RC hydraulic filter introduced for damping the peristaltic pump pulsations. The flow rate generated by the pump (Q_{pump}) is filtered by the RC hydraulic filter in order to obtain a *quasi-steady* flow rate (Q_{in}).

Figure 1

Click here to download Figure Figure1.Piola et al.,2016.png

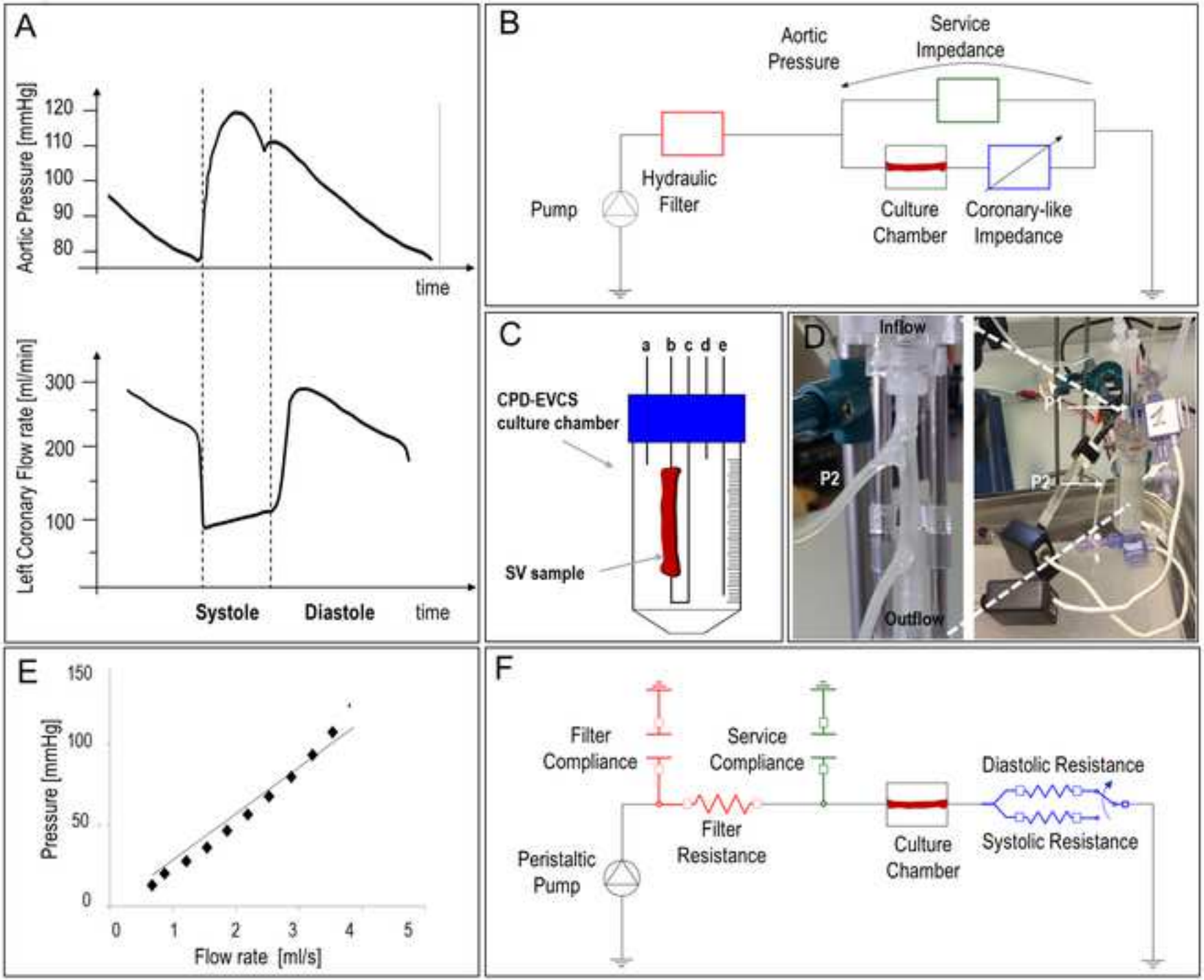

Figure 2

Click here to download Figure Figure2.Piola et al.,2016.png

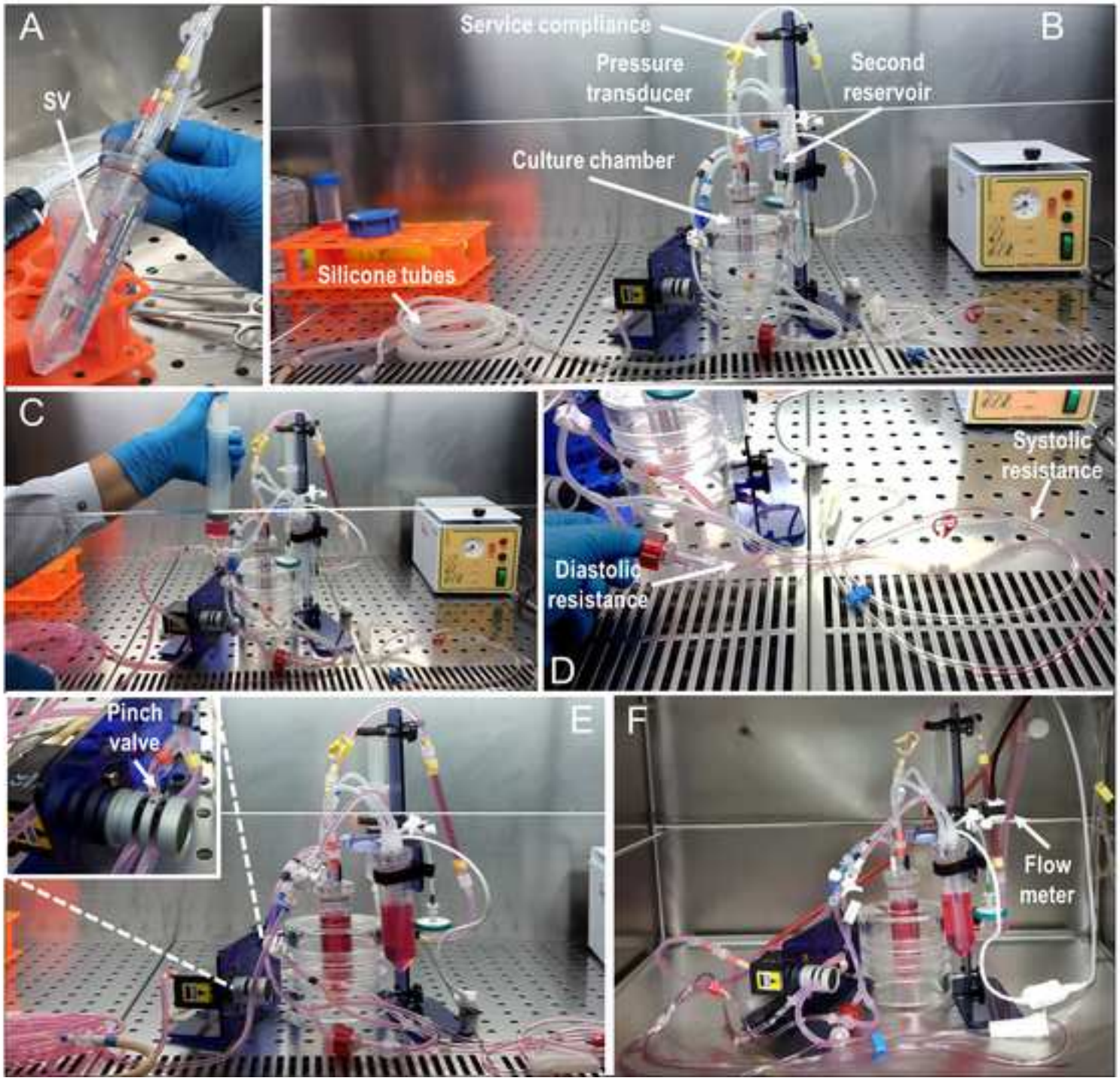

Figure 3

Click here to download Figure Figure3.Piola et al.,2016.png

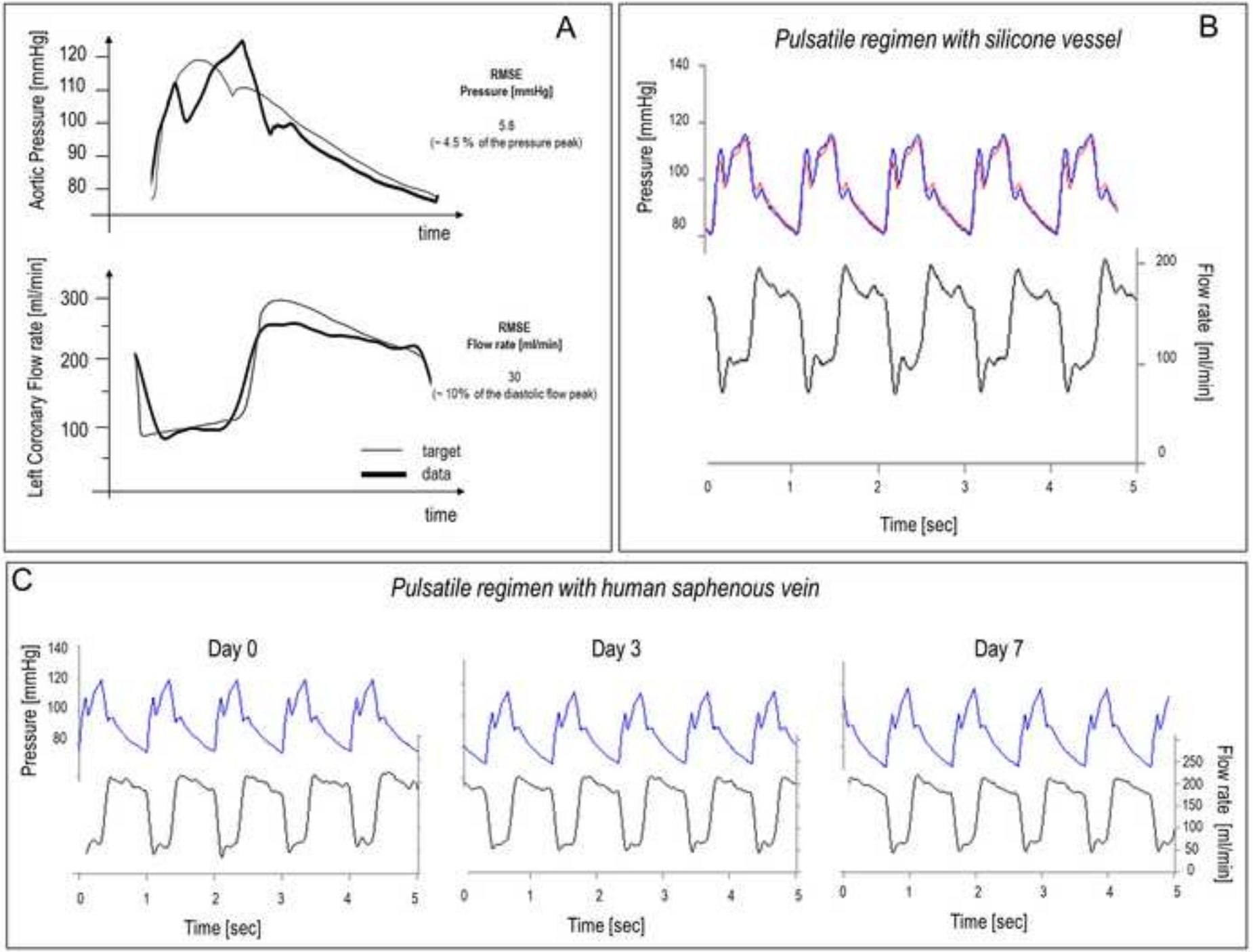

Figure 4

Click here to download Figure Figure4.Piola et al.,2016.png

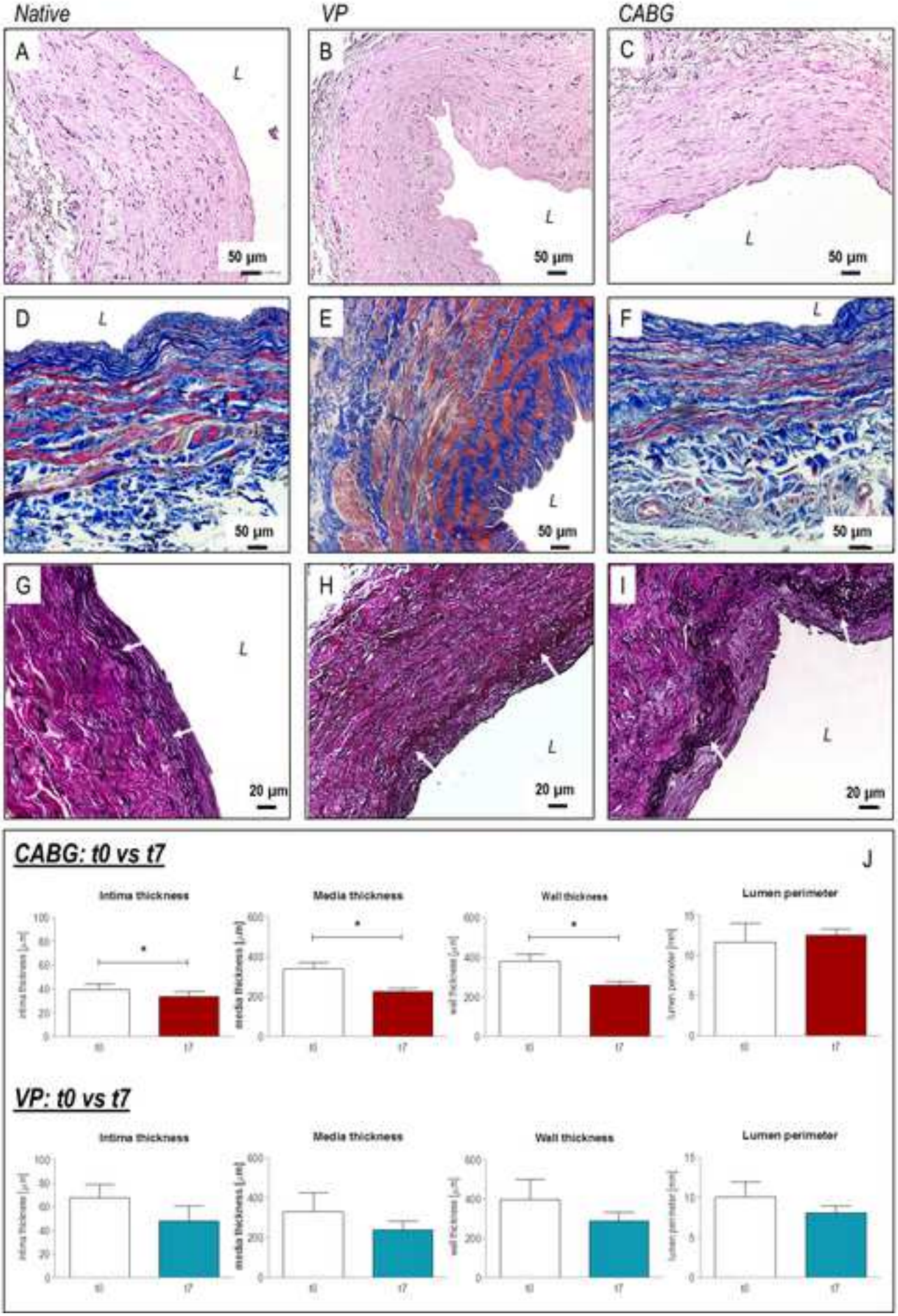

Figure 5

Click here to download Figure Figure5.Piola et al.,2016.png

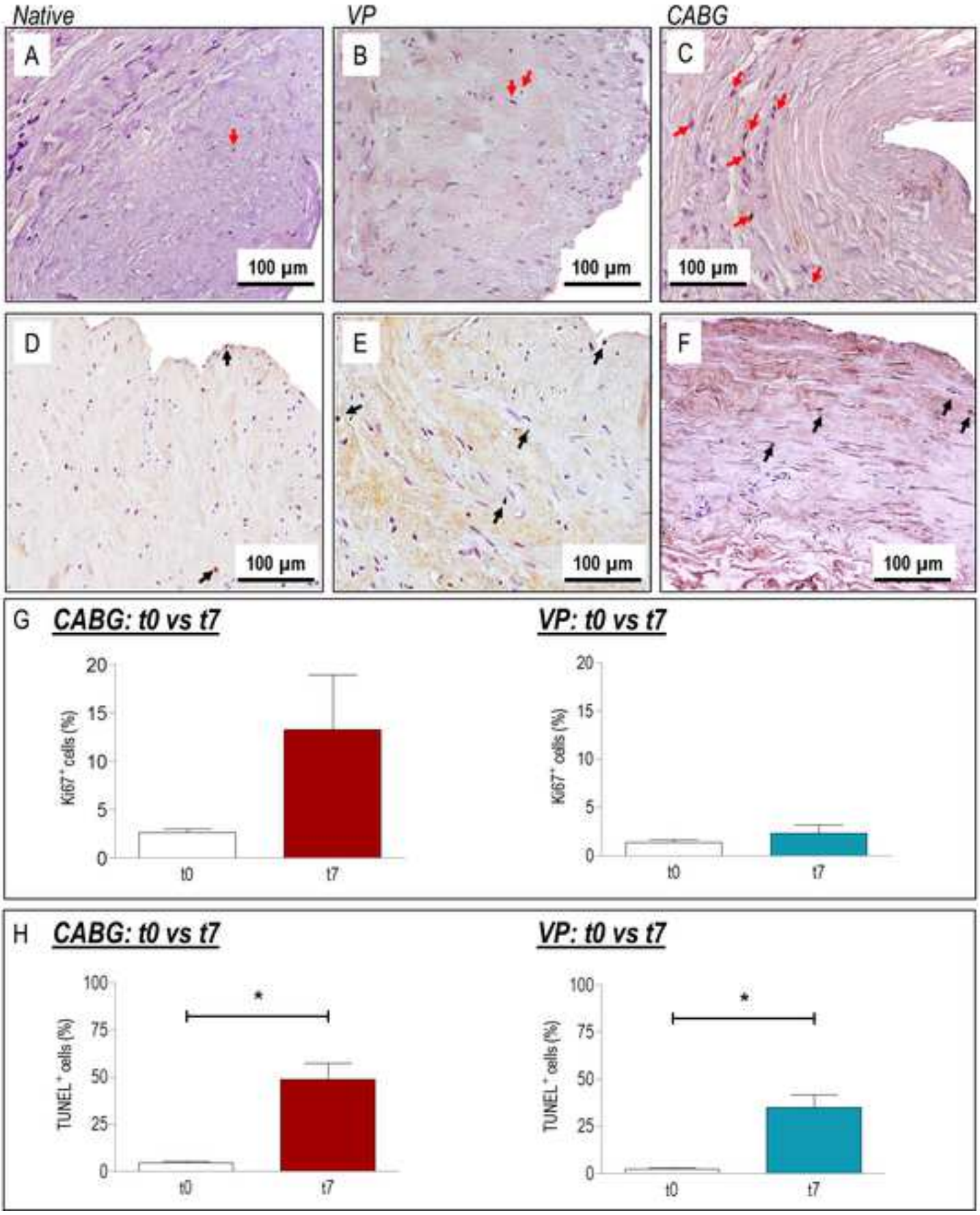

Figure 6

Click here to download Figure Figure6.Piola et al.,2016.png

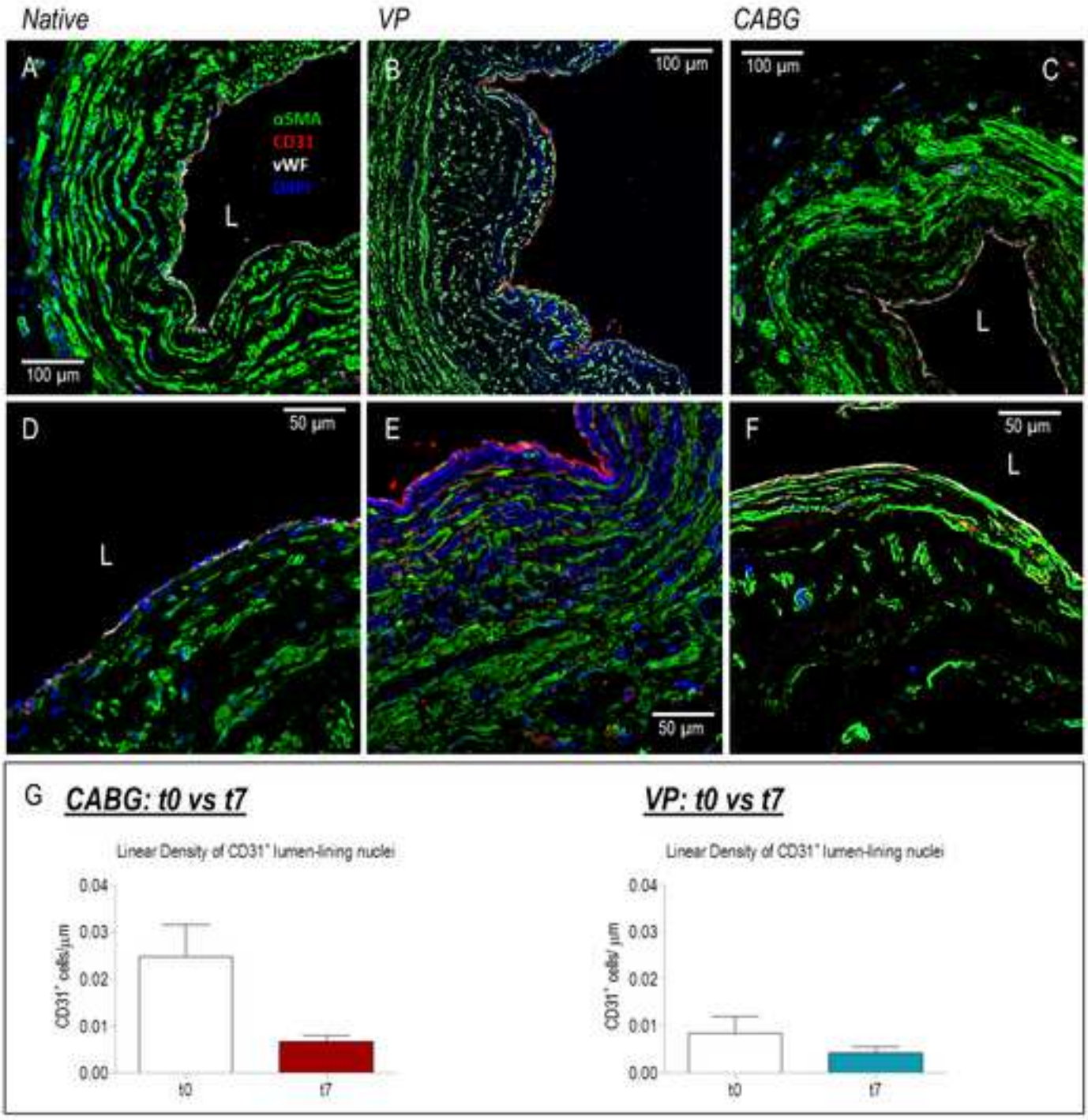

Full mimicking of coronary hemodynamics for ex-vivo stimulation of human saphenous veins

Supplementary Materials

Marco Piola[1,*,#], Matthijs Ruiter[2,#], Riccardo Vismara[1], Valeria Mastrullo[2], Marco Agrifoglio[3], Marco Zanobini[4], Maurizio Pesce[2] Monica Soncini[1] and Gianfranco Beniamino Fiore[1]

[1] Dipartimento di Elettronica, Informazione e Bioingegneria, Politecnico di Milano, , P.zza Leonardo da Vinci 32, 20133, Milan, Italy;

[2] Unità di Ingegneria Tissutale, Centro Cardiologico Monzino-IRCCS, Via Parea 4, 20138, Milan, Italy;

[3] Dipartimento di Scienze Cliniche e di Comunità, Università di Milano, Via Parea 4, 20138, Milan, Italy.

[4] Divisione Di Cardiochirurgia, Centro Cardiologico Monzino-IRCCS, Via Parea 4, 20138, Milan, Italy

# Both authors contributed equally to this work

Running title: *Ex vivo* pulsatile stimulation of human saphenous veins

*corresponding author:

Marco Piola, PhD. – Address: Politecnico di Milano, Dipartimento di Elettronica, Informazione e Bioingegneria, P.zza Leonardo da Vinci, 32, 20133 Milano, Italy, TEL: +39 02 2399 4144, FAX: +39 02 2399 3360, E-mail: marco.piola@polimi.it

1. Reference curves and values for left coronary hemodynamics – Typical flow and pressure tracings are displayed in several textbooks of medical physiology. To the purpose of our project, the curve reported in Berne's textbook[1] was used as a reference curve for the aortic pressure, *i.e.* at the inlet of the left coronary bed. Such pressure tracing well represents a typical sphygmoid pressure curve oscillating between 80 and 120 mmHg. The curve reported in Guyton's textbook[2] was used as a reference curve for left coronary flow. Such flow tracing well represents the so-called paradox behavior of coronary flow, with a relatively small systolic flow ranging about 100 ml/min and a higher diastolic flow with a peak of about 300 ml/min: an approximate 1:3 ratio which is confirmed by literature data referring to *in vivo* real time velocity measurements in the left anterior artery[3]. Concerning time-averaged flows, a reference value of 250 ml/min for the whole coronary flow is a common assumption[4], and a 70%/30% left-to-right flow repartition is widely accepted[5], which leads to a reference value of 175 ml/min for the average flow rate in the left coronary artery. The reference curves were graphically interpolated with MATLAB (The MathWorks, Inc., Natick, MA) through the Piecewise Cubic Hermite Interpolating Polynomial functions. Our experimental data were compared to the reference tracings with a root-mean-square error (RMSE) analysis to assess the performances of the system (see Fig. 3A, main text).

2. Design and working principle of the CPD system - Our CPD hydraulic system was conceived as the combination of three main sub-systems connected to the SV culture chamber and fed by an upstream peristaltic pump (refer to Figure 1B of the main text): *i*) a hydraulic filter subsystem, *ii*) a service impedance, and *iii*) a coronary-like impedance. The hydraulic filter, placed immediately after the peristaltic pump, was included to dampen the cyclical peristaltic disturbance, ensuring a relatively steady flow rate entering into the rest of the circuit. The coronary-like impedance represented the culture chamber's afterload, thus simulating the time-dependent hydraulic behavior of the coronary bed, changing periodically between a systolic and a diastolic condition. By design, both the systolic and diastolic behaviors were considered to be purely resistive, considering the hydraulic dissipative terms as the dominating contributions to replicate the coronary afterload[6, 7].

The service impedance was included to yield the desired pressure-flow dynamic behavior at the inlet of the SV hydraulic line, in the presence of a steady flow forcing term (pump + filter) with assigned periodic changes of the downstream impedance. Following is a description of the design and dimensioning of each hydraulic subsystem.

2.1 Design and dimensioning of the coronary-like impedance subsystem **-** The following relationships were used in order to determine the reference value of the diastolic and systolic time-dependent resistances (see [8, 9]):

$$V_{Syst} = 0.25\, V_{Total} = 0.25\, \bar{Q}_{Left\_Cor}\, T \tag{1}$$

$$V_{Diast} = 0.75\, V_{Total} = 0.75\, \bar{Q}_{Left\_Cor}\, T \tag{2}$$

where $\bar{Q}_{Left\_Cor}$ is the mean flow rate flowing into the left coronary artery, V_{Syst} and V_{Diast} are the blood volumes flowing during the systolic and diastolic phase, respectively, V_{Total} is the total blood volume flowing in the left coronary artery during one cardiac cycle, and T is the period of the cardiac cycle. The values of the diastolic (R_{Diast}) and systolic (R_{Syst}) resistances were calculated using the hydraulic analog of Ohm's law. Considering that the systolic interval (t_s) is approximately equal to 0.35 seconds, with simple passages, it is yielded:

$$R_{Syst} = \frac{\bar{P}_{Cor\_Syst}}{\bar{Q}_{\ Syst}} = \frac{\bar{P}_{Cor\_Syst}}{\frac{V_{Syst}}{t_s}} = 48\ \frac{mmHg\ s}{ml} \tag{3}$$

$$R_{Diast} = \frac{\bar{P}_{Cor\_\ Diast}}{\bar{Q}_{Diast}} = \frac{\bar{P}_{Cor\_Diast}}{\frac{V_{Diast}}{t_d}} = 27\ \frac{mmHg\ s}{ml} \tag{4}$$

where $\bar{P}_{Cor\_Syst}$ and $\bar{P}_{Cor\_\ Diast}$ are the mean pressures during systole (100 mmHg) and diastole (90 mmHg), while $\bar{Q}_{Syst}$ and $\bar{Q}_{Diast}$ are the corresponding mean flow rates.

The dimensioning of the coronary circuit took into account that the hydraulic resistance of the culture chamber is in series to the switching time-dependent module, as in Figure 1F (blue, main manuscript). The coronary resistances elements were realized with cell-culture compatible tubing (Tygon ND 100-65, Saint Gobain, Shore A equal to 65- medium hard). Pressure drops across the

tubing was modelled as in[10], using a fluid viscosity of 3 cP and a fluid density of 1000 kg/m^3. The length and diameter of the tubing was dimensioned according to the requirements detailed in the main text.

2.2 Design and dimensioning of the service impedance subsystem - The aim of the service impedance sub-system (green, Figure 1F, main manuscript) was to generate a sphygmoid-like pressure waveform when the whole system is forced with a constant inlet flow rate, while the resistances in the coronary branch of the CPD alternately switch between the systolic and the diastolic values. The design specifications were: *i*) minimization of the number of elements, thus making the system as compact as possible, *ii*) minimization of the priming volume of the overall circuit, and *iii*) compatibility with the use of a peristaltic pump for generating the flow. A screening among several possible solutions was carried out, involving different combinations of hydraulic resistance and/or compliance elements. The selected option was to use a single compliance element (with C=0.01 ml/mmHg) as the service impedance, which best satisfied the design requirements of compactness and low priming volume. The compliance was obtained by using a properly dimensioned air chamber. Approximating air as a perfect gas, slow replenishment up to an average working pressure (P_w) equal to 100 mmHg was modeled as an isothermal process, while compression and expansion around P_w during the working cycle were modeled as adiabatic. A volume of air of about 13.5 ml resulted to generate the desired compliance. The related hydraulic circuit component was then realized with a partially-filled 20-ml syringe. Small adjustments of the service compliance were feasible by changing the volume of the air entrapped in the syringe.

2.3 Design and dimensioning of the hydraulic filter - A low-pass RC filter was dimensioned for dampening the peristaltic pump pulsation so to feed the system with a quasi-steady flow rate (Figure S1). The fundamental frequency of the pump-generated flow oscillations (f_{noise}) was calculated as:

$$f_{noise} = \frac{n\,\omega_{rpm}}{60} \tag{5}$$

where n is the number of pump rollers, and ω_{rpm} is the pump speed (number of revolutions per minute). The filter was used to dampen flow oscillations by properly attenuating the harmonic components $\geq f_{noise}$, with the aim of obtaining a flow rate signal that well approximates a steady signal. To this purpose the cutoff frequency (f_c) of the filter was set two decades lower than the first harmonic of the noise signal ($f_c = 0.01\ f_{noise}$). The cutoff frequency is:

$$f_c = \frac{1}{2\,\pi\,\tau} = \frac{1}{2\,\pi\,R\,C} \tag{6}$$

where τ is the time constant of the RC filter, and R and C are the hydraulic resistance and compliance, respectively. A constraint on resistance R was imposed to limit the afterload pump pressure (< 300 mmHg, R equal to 120 mmHg s/ml); hence, the desired time constant was obtained by setting the filter compliance C only. The results of the dimensioning steps for Q = 175 ml/min and for different inner diameters of the pump tubes are reported in Table S1.

The filter compliance was obtained using a segment of deformable silicone tubing (Tygon 3350 Sanitary Silicone Tubing, Saint Gobain, Shore A equal to 50 – medium soft), dimensioned using the thin-walled pressure vessel theory and assuming small deformations[11]. Silicone tubing was selected in order to limit the number of components along the circuit, thus facilitating the mounting procedures under the laminar flow hood and limit the priming volume of the system. Dimensioning resulted in a silicone tube element with a length of 2500 mm, inner diameter of 3.2 mm, and wall thickness of 0.8 mm.

References

1. Berne, R. M., B. M. Koeppen,B. A. Stanton, *Berne & Levy physiology*. 6th ed.; Mosby/Elsevier: Philadelphia, PA, 2010; p xii, 836 p.
2. Guyton, A. C., *Textbook of medical physiology*. 2d ed.; W. B. Saunders Co.: Philadelphia, 1961; p 1181.
3. Chodzynski, K. J., K. Z. Boudjeltia, J. Lalmand, A. Aminian, L. Vanhamme, D. R. de Sousa, S. Gremmo, L. Bricteux, C. Renotte, G. Courbebaisse,G. Coussement, An in vitro test bench reproducing coronary blood flow signals. *Biomed Eng Online.* 14:77, 2015.
4. Ramanathan, T. S.,H. Skinner, Coronary blood flow. *Continuing Education in Anaesthesia, Critical Care & Pain.* 5:61-64, 2005.
5. Sankaran, S., M. Esmaily Moghadam, A. M. Kahn, E. E. Tseng, J. M. Guccione,A. L. Marsden, Patient-specific multiscale modeling of blood flow for coronary artery bypass graft surgery. *Ann Biomed Eng.* 40:2228-42, 2012.
6. Spaan, J. A. E., *Coronary blood flow mechanics, distribution, and control*. Kluwer Academic Publishers: Dordrecht etc., 1991; p XXIII, 389 S.
7. Downey, J. M.,E. S. Kirk, Inhibition of coronary blood flow by a vascular waterfall mechanism. *Circ Res.* 36:753-60, 1975.

8. Shaaban, A. M.,A. J. Duerinckx, Wall shear stress and early atherosclerosis: a review. *AJR Am J Roentgenol.* 174:1657-65, 2000.
9. Neuhaus, K. L., G. Sauer, H. Krause,U. Tebbe, *Video densitometric measurement of coronary flow. In: Just H, Heintzen PH, eds.Angiocardiography: current status and future developments.* Springer Verlag: New York, 1986.
10. Pennati, G., G. B. Fiore, K. Lagana,R. Fumero, Mathematical modeling of fluid dynamics in pulsatile cardiopulmonary bypass. *Artif Organs.* 28:196-209, 2004.
11. Chandran, K. B., S. E. Rittgers,A. P. Yoganathan, *Biofluid mechanics: the human circulation*. 2nd ed.; CRC Press, Taylor & Francis Group: Boca Raton, 2012; p xx, 431 pages.

RC Filter	**I.D. 3.2 mm**	**I.D. 4.8 mm**	**I.D. 6.4 mm**
ω_{rpm}	206	92	58
$f_{noise\ [Hz]}$	14	6.1	3.9
$f_{c[Hz]}$	0.14	0.061	0.039
C [ml/mmHg]	0.01	0.022	0.034
R [mmHg s/ml]	120		

Table S1. Results of the dimensioning steps for Q = 175 ml/min and for different inner diameters of the pump tubes. ω_{rpm} is the number of revolutions per minute, f_{noise} is the frequency of the noise, f_c is the cut off frequency of the RC-hydraulic filter and *I.D.* is the inner diameter of the pump tubes.

Supporting information legend of the *Video S1*

This video describes the CPD-equipped EVCS during conditioning of human SV in the incubator.